Tetrahedron 65 (2009) 4165–4172

Contents lists available at ScienceDirect

Tetrahedron

journal homepage: www.elsevier.com/locate/tet

Star-shaped oligo(fluorene ethynylene)-functionalized truxene derivatives: synthesis, characterization, and their size effects

Si-Chun Yuan [a,*], Qingjiang Sun [c], Ting Lei [b], Bin Du [b], Yong-Fang Li [c,*], Jian Pei [b,*]

[a] Department of Fundamental Science, Beijing University of Agriculture, Beijing 102206, China
[b] The Key Laboratory of Bioorganic Chemistry and Molecular Engineering of Ministry of Education, College of Chemistry and Molecular Engineering, Peking University, Beijing 100871, China
[c] Laboratory of Organic Solids, Institute of Chemistry, Chinese Academy of Sciences, Beijing 100080, China

ARTICLE INFO

Article history:
Received 18 December 2008
Received in revised form 17 March 2009
Accepted 17 March 2009
Available online 26 March 2009

ABSTRACT

A series of monodisperse, well-defined, star-shaped truxene derivatives bearing oligo(fluorene ethynylene) (OFE) branches were constructed through a convergent synthetic strategy. The radius of the largest molecule **TOFE4** was up to about 4.5 nm. Linear OFE branches with different length were first constructed in high yields alternately using the Sonogashira cross-coupling and propargyl alcohol deprotection reaction. The detailed investigation of their photophysical properties in solution and in film indicated that these star-shaped molecules exhibited obvious size effects on their distinct photoluminescence and electroluminescence behaviors. Furthermore, good performances were achieved from the fabrication of double-layer organic light-emitting diodes using these star-shaped molecules as active materials.

1. Introduction

Organic semiconductors with an extended π-conjugation system have been intensively pursued for photonics and electronics, such as organic light-emitting diodes (OLEDs),[1] organic field effect transistors (OFETs),[2] photovoltaic cells,[3] and lasers.[4] In contrast to polymers and small molecules, star-shaped molecules and dendrimers possess well-defined and uniform molecular structure as well as superior chemical purity, which still retain the solution processable and precisely designable advantage of polymers in device fabrication.[5–7] These attractive features facilitate us not only to investigate their potential application in various fields, but also to understand their unique properties, as the diameters increase and the topologies change.

The modified truxene moiety, by virtue of its unique three-dimensional topology, has become an ideal building block in the application of organic materials especially in OLED.[8] In our previous contributions, we reported some conjugated dendrimers, star-shaped molecules, and three-dimensional architectures for OLED applications.[9] Herein, we design and synthesize four monodisperse, well-defined, star-shaped truxene derivatives, **TOFE1**–**TOFE4**, as shown in Chart 1, bearing three oligo(fluorene ethynylene)[10] arms. These molecules show highly efficient greenish-blue emissions, and excellent thermal and electrochemical stabilities. Good performances are obtained from the device fabrication of OLEDs using **TOFE2**–**TOFE4** as active materials. In addition, the interesting size effect of **TOFE4** is represented and discussed. Unfortunately, in the

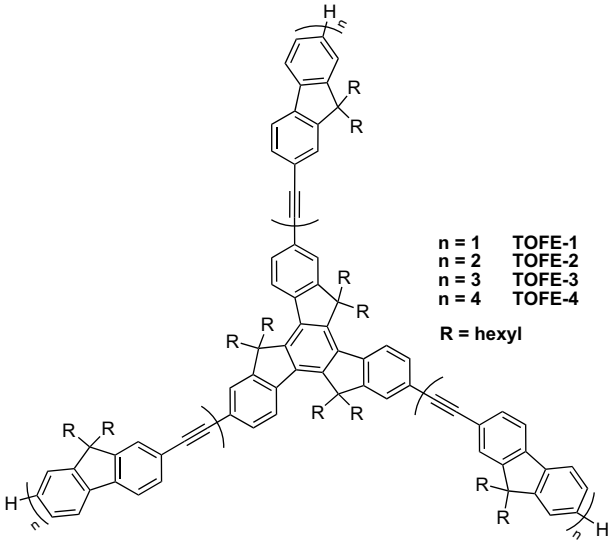

Chart 1. The structure of star-shaped molecules **TOFE1**–**TOFE4**.

* Corresponding authors. Tel./fax: +86 10 62758145.
E-mail address: jianpei@pku.edu.cn (J. Pei).

0040-4020/$ – see front matter © 2009 Elsevier Ltd. All rights reserved.
doi:10.1016/j.tet.2009.03.047

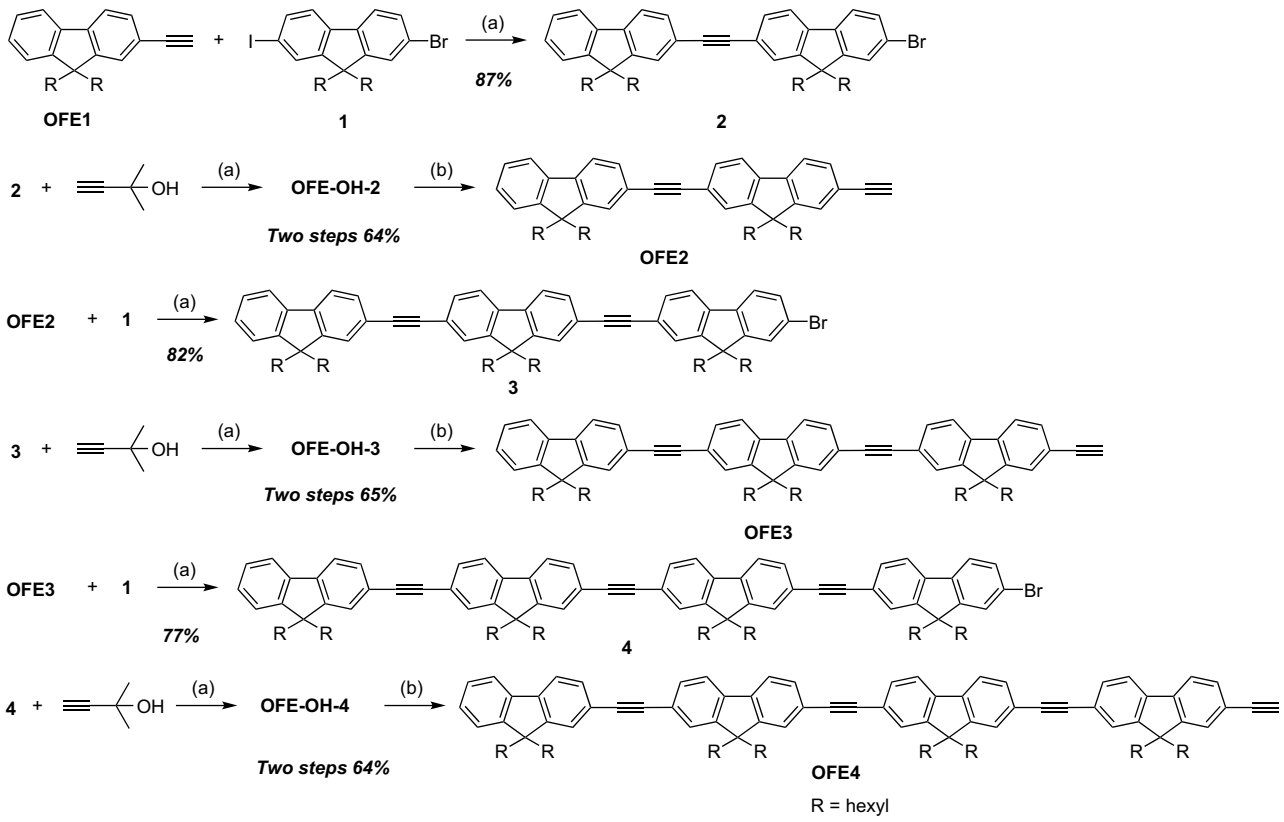

Scheme 1. Synthetic route to arms of the star-shaped molecules. Reagents and conditions: (a) $Pd(PPh_3)_2Cl_2$, CuI, Et_3N, PPh_3, THF; (b) NaOH, toluene, reflux.

preparation of this paper, Huang and co-workers reported their synthesis and preliminary device results of **TOFE1**–**TOFE3**.[8a] However, our synthetic route is different which seems more effective; furthermore, giant molecules **TOFE4** and OLED devices' results are not included in their paper.

2. Results and discussion

The general structure of oligo(fluorene ethynylene) truxenes is depicted in Chart 1. The divergent synthetic strategy of star-shaped molecules reported by our group before was not taken in this project,[9a] which was proved to give low yields and too many byproducts as the arms expand. So we first synthesized linear conjugated fluorene ethynylene oligomers, and then a Sonogashira cross-coupling reaction was implemented efficiently in good yields.

The preparation of linear oligo(fluorene ethynylene) arms (**OFE**s) started from two compounds: 2-ethynyl-9,9-dihexylfluorene (**OFE1**) and 2-bromo-9,9-dihexyl 7-iodofluorene (**1**). **OFE1** was synthesized via a Pd/Cu-catalyzed Sonogashira coupling reaction between 2-bromo-9,9-dihexylfluorene and 3-methyl-1-butyn-3-ol followed by a deprotection of the propargyl alcohol group. As illustrated in Scheme 1, the synthesis of **OFE2**–**OFE4** was processed mainly through selective Sonogashira reactions between arylethynylenes and 2-bromo-7-iodo-9,9-dihexylfluorene **1**, utilizing the different reactivities between aryl bromide and aryl iodide. Compound **1** reacting with 1 equiv of **OFE1** at room temperature selectively led to **2** in 87% yield. Through a cross-coupling reaction between **2** and 3-methyl-1-butyn-3-ol followed by a similar deprotection step, **OFE2** was obtained in 68% yield over two steps. Repetitively utilizing the Sonogashira cross-coupling and propargyl alcohol deprotection reaction smoothly afforded other two conjugated arms **OFE3** and **OFE4** in 65% and 64% yields, respectively. This strategy was different from the previous report on the synthesis of **OFE**s,[8a] and exemplified a feasible synthetic strategy for the synthesis of oligoaryl ethynylene derivatives with a satisfactory result.

Four star-shaped giant molecules were prepared as shown in Scheme 2. A Sonogashira coupling between 5,5,10,10,15,15-hexahexyl-2,7,12-triiodotruxene and 3.3 equiv of **OFE1**–**4** afforded final products **TOFE1**–**4** in 87, 75, 72, and 54% yields, respectively. In these reactions, we utilized more active $Pd_2(dba)_3$ catalyst to inhibit the homocoupling of **OFE**s and to increase the yields. As the size of **TOFE**s increases, their purification became more and more difficult, due to the similar polarity between the target molecules and the homocoupling byproducts, all of which reduced their isolated yields. All four compounds were readily soluble in common organic solvents, such as hexane, CH_2Cl_2, $CHCl_3$, THF, which allowed us to conveniently obtain their ^1H and ^{13}C NMR spectra, and MALDI-TOF MS characterization data to verify the structure and the purity of dendrimers.

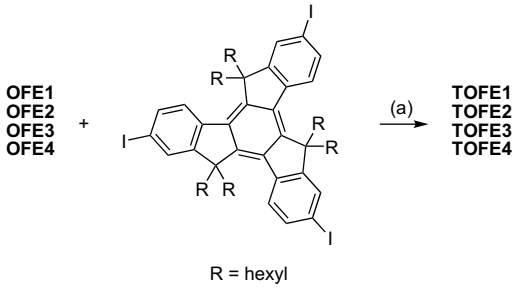

Scheme 2. Synthetic route to star-shaped molecules. Reagents and conditions: (a) $Pd_2(dba)_3$, CuI, Et_3N, PPh_3, toluene, reflux.

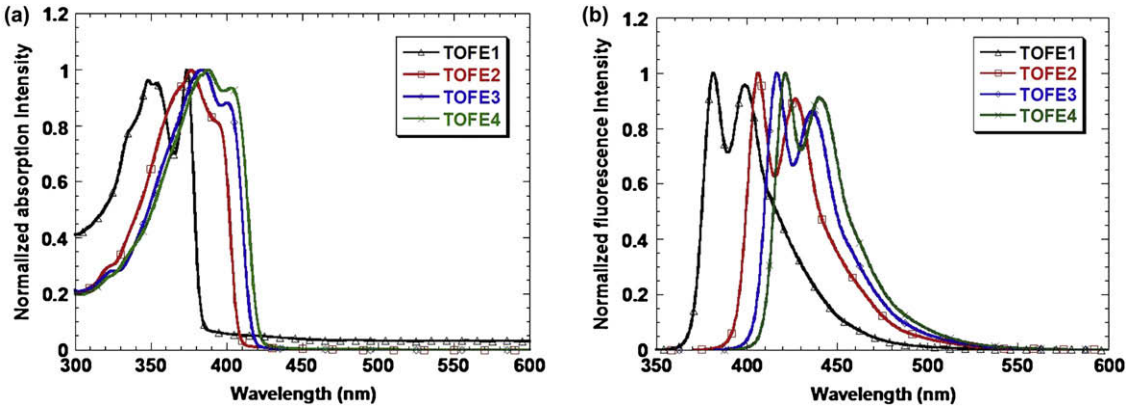

Figure 1. (a) Absorption and (b) emission spectra of **TOFE1–4** in THF solutions (1.0×10^{-6} M) at room temperature. The emission spectra were recorded using the following excitation wavelengths: 349 nm for **TOFE1**; 377 nm for **TOFE2**; 383 nm for **TOFE3**; 388 nm for **TOFE4**.

2.1. Photophysical properties in solution and in thin film

Figure 1 shows the absorption and emission spectra of **TOFE1–TOFE4** in dilute THF solutions (1.0×10^{-6} M). The absorption features of **TOFE**s with two major absorption bands were all similar with the previously reported oligo(fluorene ethynylene)s with same conjugation length.[10c] The molar extinction coefficient of the molecules was gradually enhanced as the branch lengths increased (Table 1). Their absorption maximum λ_{max} peaked at 349 nm for **TOFE1**, 377 nm for **TOFE2**, 383 nm for **TOFE3**, and 388 nm for **TOFE4**, respectively, displaying a distinct red shift as their arm lengths increased. In the emission spectra, these four molecules also showed similar behaviors as the lengths of oligo(fluorene ethynylenes) arms increased. As reported, the PL quantum efficiencies of the linear **OFE**s with 2, 3, 4, and 5 fluorene moieties were 49%, 52%, 63%, and 64%, respectively.[10c] However, the PL efficiencies of these star-shaped molecules showed obvious changes in the comparison with the **OFE** counterparts and were characterized to be 47%, 62%, 77%, and 80%, respectively. We can conclude that the star-shaped molecules could obtain high PL quantum efficiencies compared with linear molecules.

Figure 2 shows the absorption and emission spectra of **TOFE1–TOFE4** in thin films, spin coated from their THF solution (10 mg/mL). The absorption spectra of these four molecules in thin films show almost identical features as those in dilute solutions. The emission spectra of the four giant molecules displayed obvious changes compared with those in dilute solutions: First, the outlines of the spectra have changed, possibly due to the formation of aggregates or excimers in solid states. Second, all the molecules displayed a sharp red shift (60 nm for **TOFE1**; 61 nm for **TOFE2**; 51 nm for **TOFE3**; 31 nm for **TOFE4**). The excitons are delocalized in the solid state through π–π interaction and thus had a lower energy state than one localized in a single molecule.[11] Third, **TOFE4** exhibited interesting blue shift comparing with **TOFE2** and **TOFE3** in solid states. Further molecular modeling indeed shows that the possible molecular configuration of **TOFE4** has largely departured from a planar conformation, as the size increases (Fig. 3).[12] These results were attributed to the size effect of the giant molecules[13] because the increasing length of the bent conjugated arms reduced the intermolecular interactions. Table 1 summarizes their photophysical properties both in solutions and in thin films.

2.2. Thermal properties

Thermal properties of the star-shaped molecules, which were crucial for device fabrication and stability, were measured by thermogravimetric analyses (TGA) and differential scanning calorimetry (DSC). TGA results clearly indicated that all the star-shaped molecules exhibited good thermal stability without any sign of decomposition at temperature below 410 °C in an inert atmosphere (as shown in Table 1). The measurement results of the glass-transition temperatures (T_gs) of these molecules showed that **TOFE1** displayed some crystallinity at 58 °C; however, other three molecules formed amorphous in solid states.[7e,9a]

2.3. Electrochemical properties in the solid state

In the research of organic light-emitting diode materials, the relative HOMO and LUMO energetic positions are crucial in the determination of device fabrication. The HOMO and LUMO energy levels for **TOFE1–TOFE4** in solid states were estimated by conventional electrochemical techniques: cyclic voltammetry (CV) of drop cast films of **TOFE1–TOFE4** performed in CH_3CN and n-Bu_4NPF_6 was used as the supporting electrolyte. All compounds in

Table 1
Photophysical, thermal properties, of **TOFE1–4**

Compounds	λ_{abs} [nm][a] (log(ε[M^{-1} cm^{-1}])) (THF)	λ_{abs} [nm] (film)	λ_{PL}[a] [nm] (THF)	λ_{PL} [nm] (film)	Φ_F[b] (THF)	E_g[c] [eV]	T_g[d] [°C]	$T_d^{5\%}$[e] [°C]
TOFE1	349 (5.82), 374 (5.84)	351, 379	382, 399	442 (467)	47	3.25	58	411
TOFE2	377 (6.05), 394 (5.95)	380, 400	407, 427	468 (498)	62	3.04	85	418
TOFE3	383 (6.20), 401 (6.14)	388, 406	416, 437	467 (495)	71	2.97	105	426
TOFE4	388 (6.23), 403 (6.21)	390, 409	422, 440	451 (462)	80	2.95	118	427

[a] From THF solution (10^{-6} M).
[b] Φ_F was measured in THF using 9,10-diphenylanthracene (in cyclohexane, Φ_F=1.00) as reference.
[c] Bandgap estimated from the long-wavelength onset of the absorption band (in THF).
[d] Measurement by DSC at 10 °C/min.
[e] Temperature with 5% mass loss measured by TGA at 10 °C/min.

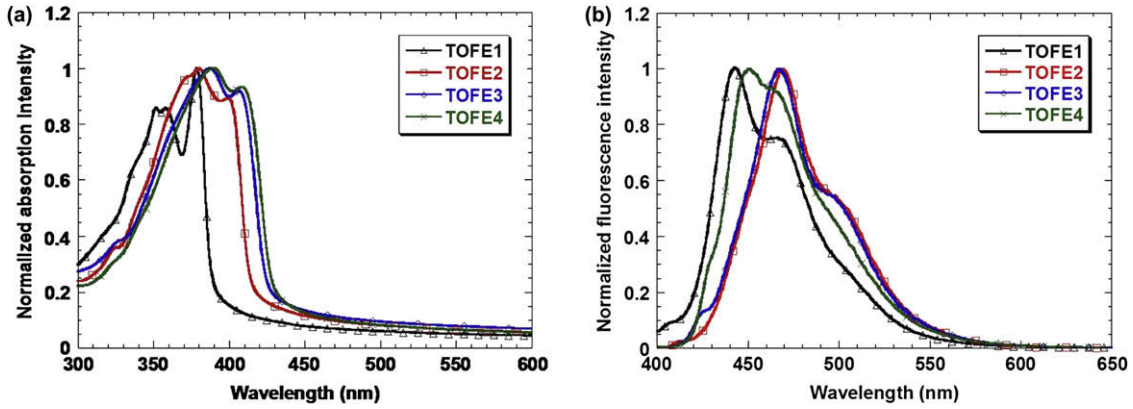

Figure 2. (a) Absorption and (b) emission spectra of **TOFE1–4** in thin films at room temperature. The emission spectra were recorded using the following excitation wavelengths: 351 nm for **TOFE1**; 380 nm for **TOFE2**; 388 nm for **TOFE3**; 390 nm for **TOFE4**.

Figure 3. Molecular model of **TOFE4**. Energy was minimized using the Merck Molecular Force Field 94 (MMFF94).

thin films showed reversible oxidation and reduction waves. Their HOMO and LUMO levels were determined using the onset positions of the oxidation peaks and the reduction peaks, respectively. As the conjugation arms expand, the oxidation of the molecules shifted negatively from 1.53 to 1.40 V, while the reduction shifted positively from −2.18 to −1.98 V. E_g^{CV} estimated from the difference between the onsets of the reduction wave and the first oxidation peak was found to vary in the range 3.38–3.71 V (Table 2), which is consistent with the UV–vis absorption spectra. HOMO and LUMO levels of these molecules were determined by the $E^{ox}{}_{1/2}$ and E_g^{CV} (HOMO=$E^{ox}{}_{1/2}$+4.4 eV; LUMO=HOMO−E_g^{CV}).

2.4. Electroluminescence

To investigate the electroluminescence properties of those materials, double-layer devices with the configuration of ITO/PEDOT:PSS/polyTPD and PVK/**TOFE**s/Ca/Al were fabricated. PVK is introduced as hole transporting and electron blocking material in OLEDs,[14a,b] in consideration of the low electron affinity (ca. 2.3 eV) and ionization potential (ca. 5.8 eV) of **TOFE**s. The hole-injection barrier from PEDOT:PSS layer to PVK one is 0.4 eV; however, that from PEDOT:PSS layer to poly-(*N*,*N*-bis(4-butylphenyl))-*N*,*N*-bis(phenyl)benzidine (polyTPD) one is only 0.1 eV, which indicated that the hole injection from the anode to polyTPD layer should be much easier than that to PVK layer. Therefore, polyTPD was doped into PVK to improve the hole-injection capabilities of the desired devices.[14c]

As shown in Figure 4, compared with its PL features in the thin film, the EL λ_{max} of **TOFE4** exhibited blue shift. The emission peaks of devices were located at 472 nm, 470 nm, and 448 nm for **TOFE2**, **TOFE3** and **TOFE4**, respectively (Fig. 4a). All in all, the EL spectra from devices are almost identical in peak position and line-width with PL emissions, where we also observed the size effect of giant molecules. The preliminary device performances are shown in Table 2. The devices turn on at a voltage of 3.7 V, 4.5 V and 5.3 V (1.0 cd/m^2) for **TOFE2**, **TOFE3**, and **TOFE4**, respectively (Fig. 4d). The maximum brightness and luminous efficiency are 5176 cd/m^2 and 0.6 cd/A achieved by **TOFE3** based devices (Fig. 4b and c).

To our best knowledge, this is the first time to investigate the EL performance of star-shaped **OFE** derivatives as active light-emitting materials. **TOFE2–TOFE4** displayed good EL performance. In comparison with devices of **TOFE2** and **TOFE3**, that of **TOFE4** exhibited lower luminous efficiency and maximum brightness, which can be

Table 2
CV data and device performances of compounds **TOFE1–TOFE4**

Compounds	E_{ox}^{onset} [V]	E_{red}^{onset} [V]	E_g[a] [V]	HOMO [eV]	LUMO [eV]	EL (nm)	fwhm (nm)	Turn-on voltage[b] (V)	CE (cd/A)	I_{max} [mA/cm]	L_{max} (cd/m^2, V)
TOFE1	1.53	−2.18	3.71	−5.83	−2.12						
TOFE2	1.47	−2.03	3.50	−5.77	−2.27	472	66	3.7	0.55	666	4618, 21
TOFE3	1.43	−2.00	3.43	−5.73	−2.30	470	67	4.5	0.60	1639	5176, 21
TOFE4	1.40	−1.98	3.38	−5.70	−2.32	448, 469	92	5.1	0.41	1163	2861, 21

[a] Bandgap estimated from the onset for the reduction and oxidation peaks.
[b] The voltage with a brightness of 1 cd/m^2.

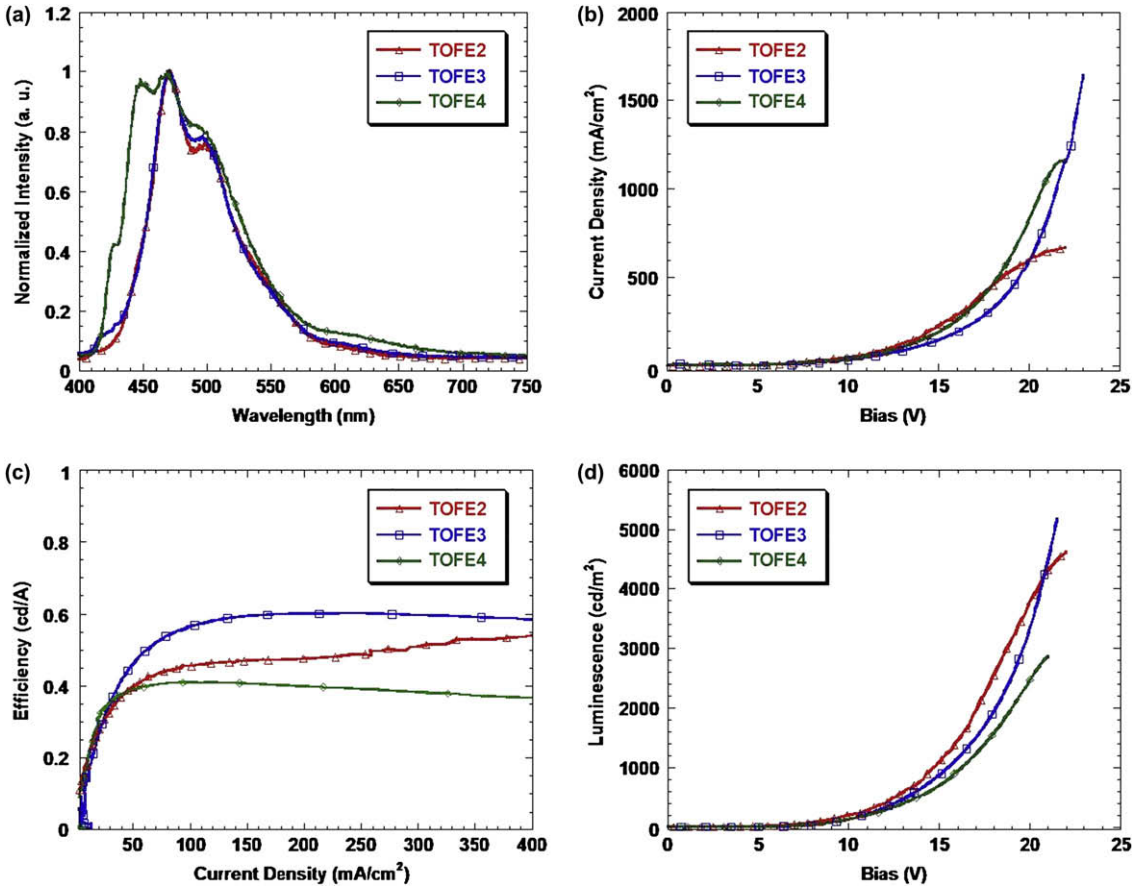

Figure 4. Electroluminescence properties of **TOFE2**–**TOFE4**; (a) normalized EL spectra; (b) current density–voltage, (c) efficiency–current density, and (d) brightness–voltage diagrams for double-layered devices.

attributed to the blue shift of EL spectra, which was in turn due to obvious self-absorption caused by the overlap of its absorption and emission spectra.

3. Conclusions

In summary, we have constructed a series of monodisperse, well-defined, star-shaped truxene derivatives bearing oligo-(fluorene ethynylene) branches, through a new convergent synthetic strategy in high yields. These star-shaped molecules represent highly efficient greenish-blue light emissions, and excellent thermal, electrochemical stabilities. Bright EL emission with good device performances is achieved from double-layer devices using **TOFE2**–**TOFE4** as the active materials. The size effect of giant molecules **TOFE4** is first investigated to reveal its different PL and EL behaviors, as well as the OLED performances. We believe that these investigations are instrumental for us to understand the optical properties and device performances of giant molecules.

4. Experiment section

4.1. General methods

All chemicals, reagents, and solvents were used as received from commercial sources without further purification except tetrahydrofuran (THF), triethylamine (Et_3N), and toluene had been distilled over sodium/benzophenone, CaH_2, and sodium, respectively. All nonaqueous operations were carried out under a dry, oxygen-free, nitrogen atmosphere. Pd/Cu-catalyzed couplings of aryl halides and terminal alkynes were conducted according to reported procedures.[15] Precursors **OFE1**,[10c,1b] compound **1**,[16] and 5,5,10,10,15,15-hexahexyl-2,7,12-triiodotruxene[11] were prepared according to literature procedures. Column chromatography was carried out on silica gel (100–200 m). ^1H and ^{13}C NMR spectra were recorded on a Mercury plus 300 MHz or Bruker 400 MHz using $CDCl_3$ as solvent and tetramethylsilane (TMS) as internal standard in all cases. Elemental analyses were carried on Elementar Vario EL (Germany). Mass spectra were obtained with a JEOL JMS-70 spectrometer in EI mode and a MALDI-TOF (matrix assisted laser desorption ionization/time-of-flight)-MS mass spectrometer Bruker BIFLEX III. UV–vis spectra were recorded on PerkinElmer Lambda 35 UV–vis spectrometer. PL spectra were carried out on Perkin-Elmer LS 55 Luminescence Spectrometer. Thermal gravity analyses (TGA) were carried out on a TA Instrument Q600 analyzer. Differential scanning calorimetry (DSC) was run on a Mettler DSC 822^e module in conjugation with a Mettler Thermal Analyst STAR^e system under a heating rate of 10 °C/min and a nitrogen flow rate of 60 cm^3/min. Cyclic voltammetry (CV) was performed using BASI Epsilon workstation and measurements were carried out in acetonitrile containing 0.1 M n-Bu_4NPF_6 as a supporting electrolyte. Carbon electrode was used as a working electrode and a platinum wire as a counter electrode; all potentials were recorded versus Ag/AgCl (saturated) as a reference electrode. The scan rate was 100 mV/s.

OLED was fabricated on pre-patterned indium-tin oxide (ITO) with sheet resistance 10–20 Ω/cm^2. The substrate was ultrasonic cleaned with acetone, detergent, deionized water, and 2-propanol. Oxygen plasma treatment was made for 10 min as the final step of substrate cleaning to improve the contact angle just before film coating. Onto the ITO glass was spin-coated a layer of PEDOT:PSS

film with thickness of 50 nm from its aqueous dispersion, to improve the hole injection and to avoid the possibility of leakage. PEDOT:PSS film was dried at 80 °C for 2 h in the vacuum oven. The solution of all materials in *p*-xylene was prepared in a nitrogen-filled drybox and spin coated on top of the ITO/PEDOT:PSS surface. Typical thickness of the emitting layer was 50–80 nm. Then a thin layer of barium as an electron injection cathode and the subsequent 200 nm thick aluminum protection layers were thermally deposited by vacuum evaporation through a mask at a base pressure below 2×10^{-4} Pa. The deposition speed and the thickness of the barium and aluminum layers were monitored by a thickness/rate meter. The cathode area defines the active area of the device. The typical active area of the devices in this study is 0.15 cm^2. The EL layer spin-coating process and the device performance tests were carried out within a glovebox with nitrogen circulation. The luminance of the device was measured with a calibrated photodiode. External quantum efficiency was obtained by the measurement of the integrating sphere, and luminance was calibrated after the encapsulation of devices with UV-curing epoxy and thin cover glass.

4.2. General methods for the preparation of linear and star-shaped oligo(fluorene ethynylene) derivatives

*4.2.1. General procedure for compounds **2–4***

To a solution of **OFE1–3** (1 equiv) and 2-bromo-7-iodo-9,9-dihexylfluorene (1.05 equiv) in a mixture of THF (20 mL/mmol) and Et_3N (6 mL/mmol) were added $Pd(PPh_3)_2Cl_2$ (0.03 equiv), PPh_3 (0.06 equiv), and CuI (0.02 equiv). After it was stirred under nitrogen atmosphere for 20 h at room temperature, the mixture was quenched with NH_4Cl. The aqueous solution was extracted with CH_2Cl_2. The combined organic extracts were washed with brine, and then dried over anhydrous $MgSO_4$. After removal of the solvents under reduced pressure, the residue was purified by column chromatography on silica gel to afford compounds **2–4**, respectively.

*4.2.2. General procedure for compounds **OFE2–4***

To a solution of compounds **2–4** (1 equiv) and 2-methyl-1-but-3-yn-3-ol (2 equiv) in a mixture of THF (20 mL/mmol) and Et_3N (6 mL/mmol) were added $Pd(PPh_3)_2Cl_2$ (0.04 equiv), PPh_3 (0.08 equiv), and CuI (0.04 equiv). After it was refluxed for 24 h, the mixture was quenched with NH_4Cl. The aqueous solution was extracted with CH_2Cl_2. The combined organic extracts were washed with brine, and then dried over $MgSO_4$. After removal of the solvents under reduced pressure, the residue was purified by column chromatography on silica gel to afford **OFEOH**. **OFEOH** was dissolved in toluene (20 mL/mmol) and then NaOH (4 equiv) was added to this solution. The mixture was refluxed for 10 h and then quenched with NH_4Cl. The aqueous solution was extracted with CH_2Cl_2. The combined organic extracts were washed with brine, and then dried over $MgSO_4$. After removal of the solvents under reduced pressure, the residue was purified by column chromatography on silica gel to afford **OFE2–4**, respectively.

*4.2.3. General procedure for compounds **TOFE1–4***

A flask with a side arm was charged with oligo(fluorene ethynylene) branches (1.1 equiv/reaction site), 5,5,10,10,15,15-hexahexyl-2,7,12-triiodotruxene (1 equiv), $Pd_2(dba)_3$ (0.02 equiv), PPh_3 (0.1 equiv), CuI (0.02 equiv), and dry Et_3N (30 mL/mmol of iodide). The flask was then evacuated and back-filled with nitrogen three times, capped and stirred at 60 °C. After completion of reaction, the reaction mixture was diluted with dichloromethane. After extraction, the combined organic layers were washed with water and brine, followed by removal of solvents. The residue was purified by flash chromatography to afford the desired product.

4.3. TOFE1

The product was obtained as pale yellow solid following the general procedure for coupling and purified by chromatography over silica gel (petroleum ether/CH_2Cl_2, 15/1). Yield: 87%. ^1H NMR ($CDCl_3$, 400 MHz, ppm): δ 8.38–8.36 (3H, d, J=8.3 Hz, Ar-H), 7.73–7.59 (m, 18H, Ar-H), 7.38–7.33 (m, 9H, Ar-H), 3.00–2.93 (6H, m, CH_2), 2.15–2.09 (6H, m, CH_2), 2.03–1.99 (12H, t, J=8.3 Hz, CH_2), 1.16–1.06 (36H, m, CH_2), 0.99–0.85 (42H, m, CH_2), 0.80–0.77 (18H, t, J=7.0 CH_3), 0.65–0.61 (24H, t, J=7.1 Hz, CH_2, CH_3), 0.53 (12H, br s, CH_2). ^{13}C NMR ($CDCl_3$, 75 MHz, ppm): δ 153.7, 151.0, 150.8, 145.9, 141.5, 140.4, 140.2, 138.0, 130.6, 129.9, 127.5, 126.9, 126.0, 125.3, 124.5, 122.9, 121.5, 121.2, 120.0, 119.7, 91.0, 90.2, 55.8, 55.2, 55.1, 40.5, 37.0, 31.5, 30.9, 29.7, 29.4, 24.0, 23.7, 22.6, 22.3, 14.0, 13.9. MALDI-TOF MS (m/z): 2022 $(M+Ag)^+$, 1830 $(M-C_6H_{13})^+$. Anal. Calcd for $C_{144}H_{186}$: C, 90.22; H, 9.78. Found: C, 90.20; H, 9.68.

4.4. 2-Bromo-7-(9,9-dihexyl-9*H*-fluorene-2-ylethynyl)-9,9-dihexyl-9*H*-fluorene (compound 2)

The product was obtained following the general procedure for coupling and purified by chromatography over silica gel (petroleum ether/CH_2Cl_2, 20/1). Yield: 89%. ^1H NMR ($CDCl_3$, 300 MHz, ppm): δ 7.71–7.64 (3H, m, Ar-H), 7.57–7.52 (5H, m, Ar-H), 7.48–7.44 (2H, m, Ar-H), 7.35–7.31 (3H, m, Ar-H), 2.00–1.93 (8H, m, CH_2), 1.16–1.04 (24H, m, CH_2), 0.80–0.74 (12H, m, CH_3), 0.62–0.60 (8H, m, CH_2). ^{13}C NMR ($CDCl_3$, 75 MHz, ppm): δ 153.2, 151.0, 150.8, 150.4, 141.4, 140.4, 140.2, 139.5, 130.7, 130.6, 130.1, 127.5, 126.9, 126.1, 125.9, 122.8, 122.1, 121.5, 121.4, 121.3, 120.0, 119.9, 119.8, 119.6, 90.9, 90.2, 55.5, 55.1, 40.5, 40.4, 31.5, 29.7, 29.7, 23.7, 22.6, 14.0. EI-MS (m/z): 770 (M^+). Anal. Calcd for $C_{52}H_{65}Br$: C, 81.61; H, 8.51. Found: C, 81.70; H, 8.65.

4.5. 2-(9,9-Dihexyl-9*H*-fluorene-2-ylethynyl)-7-ethynyl-9,9-dihexyl-9*H*-fluorene (OFE2)

The product was obtained as pale yellow solid following the general procedure. Overall yield: 68%. ^1H NMR ($CDCl_3$, 300 MHz, ppm): δ 7.72–7.63 (4H, m, Ar-H), 7.58–7.54 (4H, m, Ar-H), 7.51–7.47 (2H, m, Ar-H), 7.35–7.33 (3H, m, Ar-H), 3.16 (1H, s, C≡C–H), 2.00–1.95 (8H, m, CH_2), 1.15–0.98 (24H, m, CH_2), 0.79–0.74 (12H, m, CH_3), 0.62–0.58 (8H, m, CH_2). ^{13}C NMR ($CDCl_3$, 75 MHz, ppm): δ 151.1, 151.0, 150.8, 141.5, 141.2, 140.4, 131.2, 130.7, 130.6, 127.5, 126.9, 126.5, 125.9, 122.8, 122.3, 121.4, 120.6, 120.1, 120.0, 119.9, 119.7, 91.0, 90.3, 84.6, 77.3, 55.2, 55.1, 40.5, 40.4, 31.5, 29.7, 23.7, 22.6, 14.0. EI-MS (m/z): 714 (M^+). Anal. Calcd for $C_{54}H_{66}$: C, 90.70; H, 9.30. Found: C, 90.58; H, 9.12.

4.6. TOFE2

The product was obtained as yellow solid following the general procedure for coupling and purified by chromatography over silica gel (petroleum ether/EtOAc, 20/1). Yield: 75%. ^1H NMR ($CDCl_3$, 400 MHz, ppm): δ 8.39–8.37 (3H, d, J=8.2 Hz, Ar-H), 7.74–7.56 (m, 36H, Ar-H), 7.37–7.31 (m, 9H, Ar-H), 2.98 (6H, br s, CH_2), 2.14 (6H, br s, CH_2), 2.01–1.97 (24H, m, CH_2), 1.16–0.62 (198H, m, CH_2, CH_3). ^{13}C NMR ($CDCl_3$, 75 MHz, ppm): δ 153.7, 151.1, 151.0, 150.8, 145.9, 141.4, 140.8, 140.6, 140.4, 140.3, 138.0, 130.8, 130.6, 129.0, 127.5, 126.9, 125.9, 125.3, 124.6, 122.9, 122.1, 122.0, 121.4, 121.1, 120.0, 119.7, 90.9, 90.6, 90.4, 55.8, 55.3, 55.1, 40.6, 40.5, 37.0, 31.6, 31.5, 29.8, 29.7, 29.5, 24.0, 23.7, 22.7, 22.6, 22.3, 14.0, 13.9. MALDI-TOF MS (m/z): 3095 $(M+Ag)^+$, 2902 $(M-C_6H_{13})^+$. Anal. Calcd for $C_{225}H_{282}$: C, 90.48; H, 9.52. Found: C, 90.36; H, 9.51.

4.7. Compound 3

The product was obtained following the general procedure for coupling and purified by chromatography over silica gel (petroleum

ether/CH_2Cl_2, 20/1). Yield: 82%. ^{1}H NMR ($CDCl_3$, 300 MHz, ppm): δ 7.72–7.65 (5H, m, Ar-H), 7.59–7.53 (9H, m, Ar-H), 7.48–7.45 (2H, m, Ar-H), 7.36–7.33 (3H, m, Ar-H), 2.04–1.96 (12H, m, CH_2), 1.16–1.05 (36H, m, CH_2), 0.85–0.0.74 (18H, m, CH_3), 0.63–0.61 (12H, m, CH_2). ^{13}C NMR ($CDCl_3$, 75 MHz, ppm): δ 153.2, 151.1, 151.0, 150.8, 150.4, 141.5, 140.8, 140.6, 140.4, 140.3, 139.5, 130.7, 130.6, 130.1, 127.5, 126.9, 126.2, 125.9, 122.9, 122.1, 122.0, 121. 9, 121.5, 121.4, 121.3, 120.0, 119.8, 119.7, 90.9, 90.8, 90.7, 90.4, 55.5, 55.3, 55.1, 40.5, 40.4, 31.6, 31.5, 29.8, 29.7, 23.8, 23.7, 22.7, 22.6, 14.0. MALDI-TOF MS (m/z): 1124 (M^+). Anal. Calcd for $C_{79}H_{97}Br$: C, 84.23; H, 8.68. Found: C, 84.05; H, 8.76.

4.8. OFE3

The product was obtained as pale yellow solid following the general procedure. Overall yield: 65%. ^{1}H NMR ($CDCl_3$, 300 MHz, ppm): δ 7.72–7.63 (6H, m, Ar-H), 7.58–7.55 (8H, m, Ar-H), 7.51–7.48 (2H, m, Ar-H), 7.35–7.31 (3H, m, Ar-H), 3.16 (1H, s, C≡C–H), 2.03–1.96 (12H, m, CH_2), 1.13–1.04 (36H, m, CH_2), 0.80–0.74 (18H, m, CH_3), 0.62–0.60 (12H, m, CH_2). ^{13}C NMR ($CDCl_3$, 75 MHz, ppm): δ 151.1, 151.0, 150.8, 141.4, 141.2, 140.7, 140.6, 140.5, 140.4, 131.2, 130.7, 130.6, 127.5, 126.9, 126.5, 125.9, 122.8, 122.1, 121.9, 121.4, 120.6, 120.1, 120.0, 119.9, 119.7, 90.9, 90.8, 90.7, 90.4, 84.6, 55.2, 55.1, 40.5, 40.4, 31.6, 31.5, 29.8, 29.7, 23.7, 22.6, 14.0. MS (MALDI-TOF): 1071 (M^+). Anal. Calcd for $C_{81}H_{98}$: C, 90.78; H, 9.22. Found: C, 90.90; H, 9.33.

4.9. TOFE3

The product was obtained as yellow solid following the general procedure for coupling and purified by chromatography over silica gel (petroleum ether/EtOAc, 10/1). Yield: 72%. ^{1}H NMR ($CDCl_3$, 400 MHz, ppm): δ 8.37 (3H, br s, Ar-H), 7.75–7.57 (54H, m, Ar-H), 7.37–7.34 (9H, m, Ar-H), 2.98 (6H, br s, CH_2), 2.15–1.98 (42H, m, CH_2), 1.17–0.63 (254H, m, CH_2, CH_3). ^{13}C NMR ($CDCl_3$, 100 MHz, ppm): δ 153.7, 151.11, 151.09, 151.07, 151.0, 150.8, 145.9, 141.4, 140.7, 140.7, 140.6, 140.4, 140.3, 138.0, 130.8, 130.7, 130.6, 127.5, 126.8, 125.9, 122.8, 122.1, 122.0, 121.9, 121.4, 121.1, 120.0, 119.6, 90.9, 90.8, 90.6, 90.3, 55.8, 55.3, 55.2, 55.1, 40.5, 40.4, 37.0, 31.6, 31.5, 29.8, 29.7, 29.4, 23.9, 23.7, 22.6, 22.3, 14.0, 13.8. MS (MALDI-TOF): 4164 $(M+Ag)^+$, 3971 $(M-C_6H_{13})^+$. Anal. Calcd for $C_{306}H_{378}$: C, 90.61; H, 9.39. Found: C, 90.49; H, 9.34.

4.10. Compound 4

The product was obtained following the general procedure for coupling and purified by chromatography over silica gel (petroleum ether/CH_2Cl_2, 15/1). Yield: 77%. ^{1}H NMR ($CDCl_3$, 300 MHz, ppm): δ 7.71–7.64 (8H, m, Ar-H), 7.59–7.52 (12H, m, Ar-H), 7.49–7.45 (2H, m, Ar-H), 7.35–7.32 (3H, m, Ar-H), 2.16–1.96 (16H, m, CH_2), 1.23–1.05 (48H, m, CH_2), 0.90–0.74 (24H, m, CH_3), 0.63–0.61 (16H, m, CH_2). ^{13}C NMR ($CDCl_3$, 75 MHz, ppm): δ 153.2, 151.1, 151.0, 150.8, 150.4, 141.4, 140.7, 140.6, 140.4, 140.2, 139.4, 132.2, 132.0, 130.7, 130.6, 130.1, 128.6, 128.4, 127.5, 126.9, 126.1, 125.9, 122.8, 122.1, 122.0, 121.9, 121.5, 121.4, 121.3, 120.0, 119.8, 119.6, 90.9, 90.8, 90.7, 90.4, 55.5, 55.2, 55.1, 40.5, 40.4, 31.6, 31.5, 29.7, 29.6, 23.7, 22.6, 14.0. MS (MALDI-TOF): 1483 (M^+). Anal. Calcd for $C_{106}H_{129}Br$: C, 85.85; H, 8.77. Found: C, 85.63; H, 8.51.

4.11. OFE4

The product was obtained as pale yellow solid following the general procedure. Overall yield: 64%. ^{1}H NMR ($CDCl_3$, 300 MHz, ppm): δ 7.71–7.64 (8H, m, Ar-H), 7.59–7.55 (12H, m, Ar-H), 7.51–7.48 (2H, m, Ar-H), 7.36–7.33 (3H, m, Ar-H), 3.16 (1H, s, C≡C–H), 2.04–1.96 (16H, m, CH_2), 1.17–1.06 (48H, m, CH_2), 0.80–0.75 (24H, m, CH_3), 0.62–0.61 (16H, m, CH_2). ^{13}C NMR ($CDCl_3$, 75 MHz, ppm): 151.1, 151.0, 150.8, 141.4, 141.2, 140.7, 140.6, 140.5, 140.4, 131.3, 130.7, 130.6, 127.5, 126.9, 126.5, 125.9, 122.8, 122.1, 122.0, 121.9, 121.4, 120.6, 120.1, 120.0, 119.9, 119.7, 90.9, 90.8, 90.7, 90.4, 84.6, 55.3, 55.2, 55.13, 40.6, 40.5, 31.6, 31.5, 29.8, 29.7, 23.8, 23.7, 22.6, 14.00. MS (MALDI-TOF): 1428 (M^+). Anal. Calcd for $C_{108}H_{130}$: C, 90.83; H, 9.17. Found: C, 90.86; H, 9.34.

4.12. TOFE4

The product was obtained as yellow solid following the general procedure for coupling and purified by chromatography over silica gel (petroleum ether/EtOAc, 10/1). Yield: 54%. ^{1}H NMR ($CDCl_3$, 400 MHz, ppm): δ 8.32 (3H, br s, Ar-H), 7.74–7.56 (72H, m, Ar-H), 7.37–7.32 (9H, m, Ar-H), 2.98 (6H, br s, CH_2), 2.17–1.97 (54H, m, CH_2), 1.25–0.62 (320H, m, CH_2, CH_3). ^{13}C NMR ($CDCl_3$, 100 MHz, ppm): δ 153.7, 151.1, 151.0, 150.8, 145.9, 141.4, 140.7, 140.6, 140.4, 140.3, 138.0, 130.7, 130.5, 127.5, 126.8, 125.9, 122.8, 122.1, 122.0, 121.9, 121.4, 121.1, 119.9, 119.6, 90.9, 90.8, 90.6, 90.3, 55.8, 55.2, 55.1, 40.5, 40.4, 31.6, 31.5, 29.7, 29.4, 23.7, 22.6, 22.2, 14.0, 13.8. MALDI-TOF MS m/z: 5234 $(M+Ag)^+$, 5040 $(M-C_6H_{13})^+$. Anal. Calcd for $C_{387}H_{474}$: C, 90.68; H, 9.32. Found: C, 90.69; H, 9.24.

Acknowledgements

This work was supported by the Major State Basic Research Development Program (Nos. 2006CB921602 and 2009CB623601) from the Ministry of Science and Technology and National Natural Science Foundation of China and Beijing Natural Science Foundation (2093033).

References and notes

1. (a) Friend, R. H.; Gymer, R. W.; Holmes, A. B.; Burroughes, J. H.; Marks, R. N.; Taliani, C.; Bradley, D. D. C.; Dos Santos, D. A.; Bredas, J. L.; Logdlund, M.; Salaneck, W. R. *Nature* **1999**, *397*, 121–128; (b) Burroughes, J. H.; Bradley, D. D. C.; Brown, A. R.; Marks, R. N.; Mackay, K.; Friend, R. H.; Burn, P. L.; Holmes, A. B. *Nature* **1990**, *347*, 539–541; (c) Tang, C. W.; Van Slyke, S. A. *Appl. Phys. Lett.* **1987**, *51*, 913–915.
2. (a) Zaumseil, J.; Sirringhaus, H. *Chem. Rev.* **2007**, *107*, 1296–1323; (b) Dimitrakopoulos, C. D.; Malenfant, P. R. L. *Adv. Mater.* **2002**, *14*, 99–117; (c) Tsumura, A.; Koezuka, H.; Ando, T. *Appl. Phys. Lett.* **1986**, *49*, 1210–1212.
3. (a) Gunes, S.; Neugebauer, H.; Sariciftci, N. S. *Chem. Rev.* **2007**, *107*, 1324–1338; (b) Tang, C. W. *Appl. Phys. Lett.* **1986**, *48*, 183–185.
4. (a) Samuel, I. D. W.; Turnbull, G. A. *Chem. Rev.* **2007**, *107*, 1272–1295; (b) McGehee, M. D.; Heeger, A. J. *Adv. Mater.* **2000**, *12*, 1655–1668; (c) Tessler, N. *Adv. Mater.* **1999**, *11*, 363–370.
5. Lo, S.-C.; Burn, P. L. *Chem. Rev.* **2007**, *107*, 1097–1116.
6. Müllen, K.; Wenger, G. *Electronic Materials: The Oligomer Approach*; Wiley-VCH: Weinheim, Germany, 1998.
7. (a) Liu, Q.-D.; Lu, J.-P.; Ding, J.-F.; Day, M.; Tao, Y.; Barrios, P.; Stupak, J.; Chan, K.; Li, J.-J.; Chi, Y. *Adv. Funct. Mater.* **2007**, *17*, 1028–1036; (b) Lai, W.-Y.; Zhu, R.; Fan, Q.-L.; Hou, L.-T.; Cao, Y.; Huang, W. *Macromolecules* **2006**, *39*, 3707–3709; (c) Yang, J.-S.; Lee, Y.-R.; Yan, J.-L.; Lu, M.-C. *Org. Lett.* **2006**, *8*, 5813–5816; (d) Chen, A. C.-A.; Wallace, J. U.; Wei, S. K.-H.; Zeng, L.-C.; Chen, S. H. *Chem. Mater.* **2006**, *18*, 204–213; (e) Kanibolotsky, A. L.; Berridge, R.; Skabara, P. J.; Perepichka, I. F.; Bradley, D. D. C.; Koeberg, M. *J. Am. Chem. Soc.* **2004**, *126*, 13695–13702; (f) Li, B.-S.; Li, J.; Fu, Y.-Q.; Bo, Z.-S. *J. Am. Chem. Soc.* **2004**, *126*, 3430–3431; (g) Zhou, X.-H.; Yan, J.-C.; Pei, J. *Org. Lett.* **2003**, *5*, 3543–3546; (h) Katsis, D.; Geng, Y. H.; Ou, J. J.; Culligan, S. W.; Trajkovska, A.; Chen, S. H.; Rothberg. *Chem. Mater.* **2002**, *14*, 1332–1339.
8. (a) Chen, Q.-Q.; Liu, F.; Ma, Z.; Peng, B.; Wei, W.; Huang, W. *Chem. Lett.* **2008**, *37*, 178–179; (b) Lai, W.-Y.; Xia, R.; He, Q.-Y.; Levermore, P. A.; Huang, W.; Bradley, D. D. C. *Adv. Mater.* **2008**, *20*, 1–6; (c) Jiang, Y.; Wang, L.; Zhou, Y.; Cui, Y.-X.; Wang, J.; Cao, Y.; Pei, J. *Chem. Asian J.* **2009**. doi:10.1002/asia.200800329; (d) He, Q-Y.; Lai, W.-Y.; Ma, Z.; Chen, D.-Y.; Huang, W. *Eur. Polym. J.* **2008**, *44*, 3169–3176; (e) Zhang, W.-B.; Jin, W.-H.; Zhou, X.-H.; Pei, J. *Tetrahedron* **2007**, *63*, 2907–2914; (f) Cao, X.-Y.; Liu, X.-H.; Zhou, X.-H.; Zhang, Y.; Jiang, Y.; Cao, Y.; Cui, Y.-X.; Pei, J. *J. Org. Chem.* **2004**, *69*, 6050–6058.
9. (a) Cao, X.-Y.; Zhang, W.-B.; Wang, J.-L.; Zhou, X.-H.; Lu, H.; Pei, J. *J. Am. Chem. Soc.* **2003**, *125*, 12430; (b) Duan, X.-F.; Wang, J.-L.; Pei, J. *Org. Lett.* **2005**, *7*, 4071–4074; (c) Luo, J.; Zhou, Y.; Niu, Z.-Q.; Zhou, Q.-F.; Ma, Y.; Pei, J. *J. Am. Chem. Soc.* **2007**, *129*, 11314–11315.
10. (a) Zeng, X.-S.; Wang, C.-S.; Bryce, M. R.; Batsanov, A. S.; Sirichantaropass, S.; García-Suárez, V. M.; Lambert, C. J.; Sage, I. *Eur. J. Org. Chem.* **2007**, *31*, 5244–5249; (b) Zhao, Z.-Z.; Xu, X.-J.; Jiang, Z.-T.; Lu, P.; Yu, G.; Liu, Y.-Q. *J. Org. Chem.* **2007**, *72*, 8345–8353; (c) Lee, S. H.; Nakamura, T.; Tsutsui, T. *Org. Lett.* **2001**, *3*, 2005–2007.

11. Schwab, A. D.; Smith, D. E.; Rich, C. S.; Young, E. R.; Smith, W. F.; de Paula, J. C. *J. Phys. Chem. B* **2003**, *107*, 11339–11345.
12. Molecular modeling was performed using ChemBio3D Ultra (version 11.0) software available from CambridgeSoft. Energy was minimized using the Merck Molecular Force Field 94 (MMFF94) (Convergence criteria: atomic root mean square force 0.01 kcal/mol; steric energy: 903.946 kcal/mol).
13. Size effects have been observed in various fields: (a) Fu, H.-B.; Yao, J.-N. *J. Am. Chem. Soc.* **2001**, *123*, 1434–1439; (b) Wang, X.; Sandman, D. J. *Macromolecules* **2008**, *41*, 773–778.
14. (a) Yang, R.-Q.; Tian, R. Y.; Yan, J.-A.; Yang, J.; Hou, Q.; Yang, W.; Zhang, C.; Cao, Y. *Macromolecules* **2005**, *38*, 244–253; (b) Hou, Q.; Zhou, Q. M.; Zhang, Y.; Yang, W.; Cao, Y. *Macromolecules* **2004**, *37*, 6299–6305; (c) Zhou, Yi; Sun, Q.; Tan, Z.; Zhong, H.; Yang, C.; Li, Y. *J. Phys. Chem. C* **2007**, *111*, 6862–6867.
15. (a) Maya, F.; Tour, J. M. *Tetrahedron* **2004**, *60*, 81–92; (b) Yuan, S.-C.; Chen, H.-B.; Zhang, Y.; Pei, J. *Org. Lett.* **2006**, *8*, 5701–5704; (c) Wang, J. L.; Yan, J.; Tang, Z.-M.; Xiao, Q.; Ma, Y.-G.; Pei, J. *J. Am. Chem. Soc.* **2008**, *130*, 9952–9962.
16. Zhang, W.; Cao, X.-Y.; Zi, H.; Pei, J. *Org. Lett.* **2005**, *7*, 959–962.